Onset of self-breakdown in a low-pressure spark gap

E. J. Lauer, S. S. Yu, and D. M. Cox
Lawrence Livermore National Laboratory, University of California, Livermore, California 94550
(Received 25 August 1980)

Conditions for self-breakdown are studied with a time-dependent one-dimensional model which includes effects of ionization by electrons, ions, and energetic neutrals, charge exchange, secondary-electron emission from the cathode due to impact of ions and neutrals, and backscattering of electrons from the anode. Theoretical predictions for the low-pressure branch of the Paschen curve are reported. *Pd* scaling is explicitly verified. In addition, the rates for current buildup above the critical pressure are calculated. The relative importance of various physical effects on the onset of self-breakdown are studied.

I. INTRODUCTION

This report presents a model for self-breakdown of low-pressure spark gaps (i.e., breakdown without the application of an external trigger).[1] The model is similar to the Townsend model of breakdown at high pressure with the important difference that E/P (electric field/gas pressure) is so high that the electrons and ions are in the runaway regime, and the high-pressure model of mean kinetic energies which are functions of E/P is not pertinent. At the onset of breakdown the electron and ion currents are low, and the distortion of the uniform electric field due to space-charge effects can be neglected. Calculations of the critical conditions for breakdown under these conditions have been published by Dempster,[2] Grarzow and McClure[3] and Bhasavanich and Parker.[4] The present treatment differs from previous work in that we employ a time-dependent treatment. The atomic processes that take place in the gap and at the electrodes together with the associated electron and ion currents are followed in time. Hence we are able to calculate the rate of growth or decay of the currents.

The basic physical processes included in the present calculation are the following:

(1) Gas ionization by electrons emitted from the cathode;

(2) Secondary electron emission at the cathode by ion impact;

(3) Gas ionization by electrons from the distributed (gas) source;

(4) Gas ionization by ions;

(5) Fast neutral formation via charge exchange;

(6) Gas ionization by fast neutrals;

(7) Secondary electron emission at the cathode by fast neutral impact;

(8) Backscatter of electrons from the anode;

(9) Gas ionization by backscattered electrons.

In constructing models for the low-pressure branch of the Paschen curve, one naturally tries the simplest thing first, i.e., just processes (1) and (2) in the above list. This model would require a cathode secondary electron coefficient per ion incident at least tenfold larger than the typical measured values. Dempster[2] first noticed this paradox; we discovered it independently.

The model calculation presented in this paper is one dimensional (1*D*). The effects of finite geometry, fringe effects, and localized phenomena, such as hot spots, are automatically excluded in this 1*D* treatment.

In Sec. II, the theoretical formulation of the problem will be presented. Numerical results from SPARKY, a 1*D* code (in x and t), based on the theory of Sec. II will be presented in Sec. III. Some details of the calculation of charge exchange and backscatter are given in Appendices A and B. The complete set of equations solved by SPARKY is summarized in Appendix C.

II. THEORY

The onset of self-breakdown is the net result of several physical processes which take place simultaneously in the gap and at the two electrodes. Initially, electrons are released from the cathode by a weak trigger which may be random or externally imposed. In the pressure range of interest, the gas density is low enough so that the acceleration of electrons toward the anode is nearly "free-fall," and yet high enough so that a few electron-ion pairs are created by direct ionization along the way. The positive ions thus created move in the opposite direction, generating secondary electrons as they impinge upon the cathode surface, thus restarting the cycle. If there are sufficient returning ions, electron emission will grow as a function of time, leading eventually to sparking across the gap. On the other hand, if the ions returning are too few, electron emission will decay with time, and the current dies out.

To calculate the number of returning ions cor-

rectly, one must, of course, take into consideration that the electrons and ions created in the gas in turn ionize as they move across the gap. The movement of the ions and electrons, the ionization process in the gap, and the secondary electron emission at the cathode are taking place continuously and must be followed self-consistently.

Two additional processes enhance the breakdown. Firstly, the ions may charge exchange with gas atoms and molecules, resulting in a shower of fast neutrals moving towards the cathode, augmenting both the ionization in the gas, as well as the secondary electron emission, as they impinge upon the electrode surface. Secondly, electrons arriving at the anode may backscatter. The backscattered electrons are quite effective at further ionization because of their lower kinetic energies. Both of these effects are included in this calculation.

The key parameter of interest in the present formulation is $I(t)$, the rate of electron emission from the cathode surface as a function of time, in units of s^{-1}. In order to calculate $I(t)$, it is convenient to introduce two auxiliary parameters, $R_i(t,x)$, the rate of creation of electrons per unit time per unit distance at position x in the gap, and $R_0(t,x)$, the corresponding rate for the creation of fast neutrals. The units of $R_i(t,x)$ and $R_0(t,x)$ are $s^{-1}\,cm^{-1}$. Since electrons and ions are always created in pairs, $R_i(t,x)$ is also the rate of creation of ions. Our objective is to write down equations which relate $I(t)$, $R_i(t,x)$, and $R_0(t,x)$ in terms of atomic cross sections and rates. Before we go into the details, we note that the present formulation permits the description of events in the gap in terms of two production rates, R_i and R_0, which are functions of only two variables, t and x. This represents a significant simplification over a more conventional Boltzmann approach where a full description of the gap physics would require at least three parameters: the distribution functions for the electrons, the ions, and the fast neutrals, respectively. Each would be a function of three variables t, x, and the velocity v. The simplification is possible because of some approximations which are justifiable under the particular conditions of the problem.

A. Electrons and ions only

We will start with the simplest case where the effects of neutrals and backscatter are excluded.

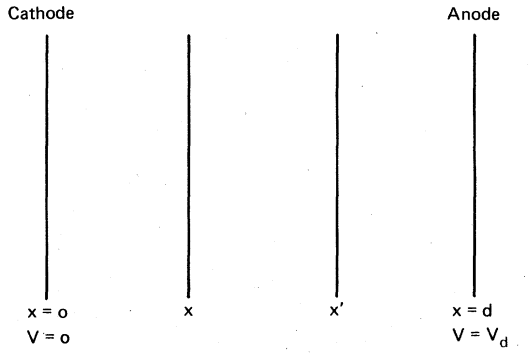

FIG. 1. Model geometry.

Three approximations are made regarding the electron and ion motion.

(1) Electrons and ions are created at rest. The assumption that ions are created at rest is clearly a good one. The initial kinetic energy of secondary electrons resulting from ionization processes are in the few eV to tens of eV regime, and small on a scale set by the potential across the gap (many kV).

(2) Space-charge effects are negligible at the start of current buildup, so we have the (uniform) vacuum E field.

(3) Atomic collisions have a negligible effect on particle kinetic energy.

For an ion created at time t' and position x', these three approximations allow us to predict the time delay to reach position x (see Fig. 1) as

$$t_i = (t - t') = \left(\frac{2Md(x' - x)}{eV_d}\right)^{1/2}, \tag{1}$$

where M is the ion mass, d the gap distance, and V_d the potential across the gap in Gaussian units. The kinetic energy of the ion at this point is

$$T_i = \frac{eV_d}{d}(x' - x). \tag{2}$$

Similar equations can be written for the time delay and energy of the electron. However, since the electron is much lighter, the time of flight is much shorter, and the flight of electrons across the gap may be assumed to take place instantaneously.

The rate of creation of electrons in the gap is then given by

$$R_i(t,x) = I(t)n_g\sigma_e\left(\frac{eV_d x}{d}\right) + \int_{x'=0}^{x} dx' R_i(t,x')n_g\sigma_e\left(\frac{eV_d}{d}(x - x')\right) + \int_{x'=x}^{d} dx' R_i(t - t_i, x')n_g\sigma_i(T_i), \tag{3}$$

where n_g is the gas density and σ_e and σ_i are the ionization cross sections due to electron impact and ion impact, respectively.

The right-hand side of Eq. (3) consists of three terms. The first term is due to ionization by electrons emitted from the cathode, the second term represents ionization by electrons created in the gap to the left of x, while the third term gives contributions from ions created earlier (at $t'=t-t_i$) at points x' to the right of x.

$I(t)$, the rate of electron emission at the cathode surface, is related in turn to the rate of ion generation in the gap by

$$I(t)=\int_{x'=0}^{d} dx' R_i(t-t_i,x')\gamma(T_i)+S(t)\,, \tag{4}$$

where $\gamma(T_i)$ is the coefficient for secondary-electron emission due to the impact of an ion with energy T_i. $S(t)$ represents an external source. The two coupled equations (3) and (4) form a closed system, which can be solved numerically for $I(t)$ and $R_i(t,x)$.

B. Effects of fast neutrals

We next include charge-exchange processes and the subsequent effects of the fast neutrals. Our formulation of the problem is based on two observations regarding charge-exchange cross sections.

(1) At low ion energies ($T_i \lesssim 10$ keV), the charge-exchange cross section σ_c is nearly independent of energy. This means that the mean free path for charge exchange is nearly position independent:

$$\lambda_0=\frac{1}{n_g\sigma_c}\,. \tag{5}$$

For situations where the ions can attain much higher energies, the constant–mean-free-path assumption is no longer valid, and a separate treatment must be introduced. This is done in Appendix A.

(2) The products of a charge-exchange collision are a fast neutral and a slow ion. In our model, we assume the ion to be at rest after a charge-exchange process, while the neutral has all the kinetic energy of the incident ion. Since charge exchange is assumed to take place with a constant mean free path, neutrals will be created with a fixed kinetic energy

$$T_0=eV_d\frac{\lambda_0}{d}\,. \tag{6}$$

The time delay between the creation of an ion at rest and the charge exchange is given by

$$t_0=\left(\frac{2Md\lambda_0}{eV_d}\right)^{1/2}. \tag{7}$$

In this mean-free-path approximation, the rate of production of neutrals is given by

$$R_0(t,x)=\sum_{m=1}^{M} R_i(t-mt_0,x+m\lambda_0)\,,$$

$$M<\frac{d-x}{\lambda_0}\leq M+1\,. \tag{8}$$

The index $m-1$ represents the number of charge exchanges a positive charge experienced prior to reaching the position x.

Introduction of neutrals affects the previous results in several ways. First, the neutrals impinging upon the cathode surface will enhance the rate of secondary electron emission. A contribution from the neutrals must be added to Eq. (4) in the form of

$$\gamma(T_0)\int_{x'=0}^{d} dx' R_0\left(t-\frac{x'}{v_0},x'\right), \tag{9}$$

where $v_0=(2T_0/M)^{1/2}$ is the speed of the neutrals.

Secondly, the neutrals can ionize the background gas, and its contribution to the electron production rate must be added to Eq. (3). The additional term is given by

$$\int_{x'=x}^{d} dx' R_0\left(t-\frac{x'-x}{v_0},x'\right) n_g\sigma_0(T_0)\,, \tag{10}$$

where σ_0 is the ionization cross section due to neutral impact.

And, thirdly, since charge exchange changes the ion energy from T_0 to zero, the ion motion across the gap is significantly altered. Whereas in the previous case without the neutrals, ions traveled in free-fall trajectories across the gap, the introduction of charge exchange leads to "sawtooth" ion velocities, with periods of constant acceleration followed by sudden drops in velocity at intervals of λ_0. This means that the ion time delay t_i and ion energy T_i in Eqs. (3) and (4) must be modified. Thus, in the presence of charge-exchange processes, we have

$$t_i=mt_0+\left(\frac{2Md}{eV_d}(x'-x-m\lambda_0)\right)^{1/2}, \tag{11}$$

where the index m is defined by

$$m\lambda_0\leq x'-x<(m+1)\lambda_0$$

and

$$T_i=\frac{eV_d}{d}(x'-x-m\lambda_0)\,. \tag{12}$$

C. General

Finally, the effects of backscatter must be included. An electron impinging upon the anode surface has a finite probability of reemerging into the gap after multiple scattering in the electrode. The energy at which the electron reemerges is not unique since inelastic collisions in the elec-

trode lead to energy loss. Furthermore, the electrons will reemerge with some angular spread. The trajectories of the backscattered electrons are parabolic. In calculating the effects of backscatter, one must integrate over these finite distributions in energy and angle of reflected electrons. This is done in Appendix B. The net effect of the backscatter is to further augment the electron creation. This is described by two additional terms in Eq. (3), one term for the backscatter of electrons originally emitted from the cathode, and one term for the electrons created in the gap, given by

$$I(t)n_g F\left(eV_d, \frac{eV_d}{d}(d-x)\right) + \int_0^x dx' R_i(t,x') n_g F\left(\frac{eV_d}{d}(d-x'), \frac{eV_d}{d}(d-x)\right), \tag{13}$$

where

$$F(T',T) = \frac{4\pi}{T'} \int_T^{T'} du \left(\frac{u-T}{u}\right) \sigma_e(u-T)\eta\left(\frac{u}{T'}\right).$$

η is a measured reflection coefficient.

In Appendix C, we write down the entire set of equations solved by the Lawrence Livermore National Laboratory code SPARKY. The effects of backscatter as well as the generalized treatment of charge exchange described in Appendix A are included in these equations.

The actual numerical integration was performed on a set of equations transformed from Eqs. (C1) through (C3) by the introduction of a new independent variable

$$z = \ln\left(\frac{x}{\kappa} + 1\right),$$

where κ is a constant. This transformation makes the evaluation of the terms due to electron-impact ionization much more tractable. In Eqs. (C1) through (C3), the important contributions to the integrals involving σ_e come from highly localized regions in x' because of the narrow width of σ_e. The transformation "spreads out" the important regions of integration thus easing the requirement on grid size in evaluating the integrals.

As a concrete example, we present calculations for the case of H_2 gas. The atomic data used are summarized below:

γ = coefficient for secondary-electron emission. For H_2^+ and for H_2^0 we used the energy dependence of H_2^+ on outgassed molybdenum.[5] The curve was adjusted upward to a maximum of 6.5 (for $\gamma \equiv \gamma_0$) instead of the original 3.0 so as to model a cathode that was *not* outgassed.[6]

σ_e = total cross section for ionization of H_2 by electron impact.[7]

σ_i = total cross section for ionization of H_2 by H_2^+ impact.[8]

σ_0 = total cross section for ionization of H_2 by H_2 impact; we used the same curve as for σ_i above.

σ_c = charge exchange cross section for H_2^+ in H_2.[9]

η = electron backscattering coefficient. We used Fig. 7 of Ref. 10 for platinum, where $\eta \equiv N(137°)/(-\cos 137°)$.

In the ionization of H_2 gas molecules, about 0.94 of the resultant ions are H_2^+ and 0.06 are H^+. In the subsequent actions of the ions (electron capture, gas ionization, and γ effect), we treated all the ions as if they were H_2^+.

Photon effects have been neglected. Collisions of electrons, energetic positive ions, and energetic neutral molecules with gas molecules would produce excited molecules at about the same rate as for the production of ionization. When the excited molecules decay, the resultant photons would release some photoelectrons from the cathode. The number of electrons released from the cathode-per-photon incident (γ_p), has a maximum of about 0.1 at a photon energy of 15 to 20 eV.[11] This is to be compared with γ_i and γ_0 which have maxima of about 6 to 12 at a heavy particle kinetic energy of about 50 keV. Thus the γ_p process is much less important than the γ_i and γ_0 processes.

III. RESULTS AND DISCUSSION

We will first present the results from one sample run of SPARKY at a gap voltage of 10 kV, a gap distance of 2.5 cm, and at 0.2 Torr H_2. In Fig. 2, we show the electron production rate R_i as a function of position x at different times. At time $t = 0$, an external source was turned on.

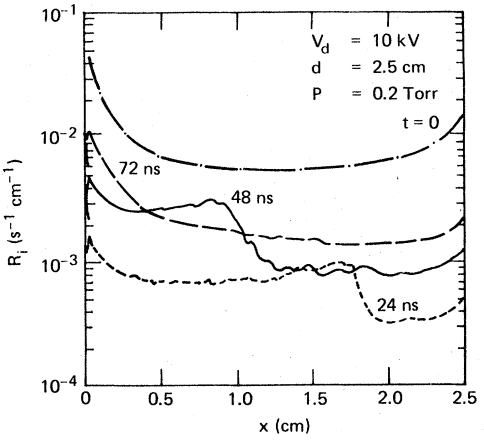

FIG. 2. Rate of electron-ion pair production versus position.

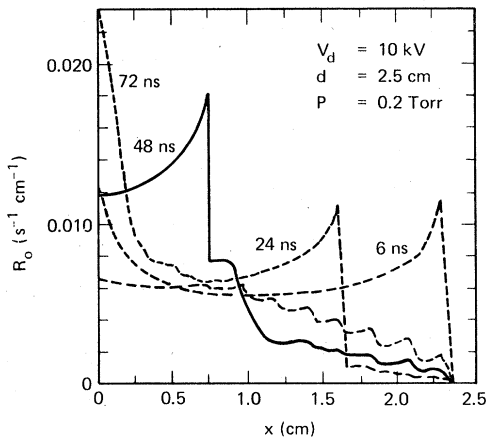

FIG. 3. Rate of neutral production versus position.

Initially, the major contribution to R_i comes from ionization by electrons emitted directly from the cathode. The shape of R_i resembles the electron ionization cross section. Since the peak of the cross section occurs below 100 eV, the peak of R_i occurs close to the cathode. We see also from the curve, deviations of R_i from σ_e away from the cathode, where the effects of ionization by secondary electrons produced in the gap dominate. This effect is augmented by the backscattered electrons which are most important at the anode, hence, the rise in R_i close to the anode. At $t=0$, there is no effect due to neutrals. At a later time, $t=24$ ns, the external source has been turned off; and hence, we see a significant reduction in R_i. The ions which were created while the source was on now move towards the cathode. The "edge" at around $x=1.75$ cm marks the position of the first generation ions produced at the anode while the source was still on. This sharp edge continues to move to the left at a speed which corresponds to the rate of ion transit across the gap as can be seen in the curve at 48 ns. At $t=72$ ns, all the first generation ions have reached the cathode, and R_i settles into a quasiequilibrium, with the shape of R_i remaining relatively unchanged beyond this time. The "equilibrium" shape of R_i shows characteristically two peaks, one close to the cathode corresponding to the peak of direct electron ionization, and a less prominent one at the anode, corresponding to the effects of backscattered electrons. Figure 3 plots the corresponding neutral production rates R_0. One sees an even more prominent feature of a sharp edge moving to the left. The plots of R_0 show some sawtooth structures, with periodicities equal to the collision length for charge exchange. This structure is a result of the mean-free-path

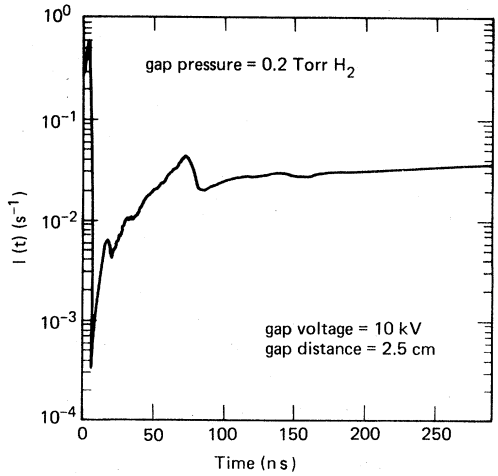

FIG. 4. Rate of electron emission from the cathode versus time (at 10 kV and 0.2 Torr).

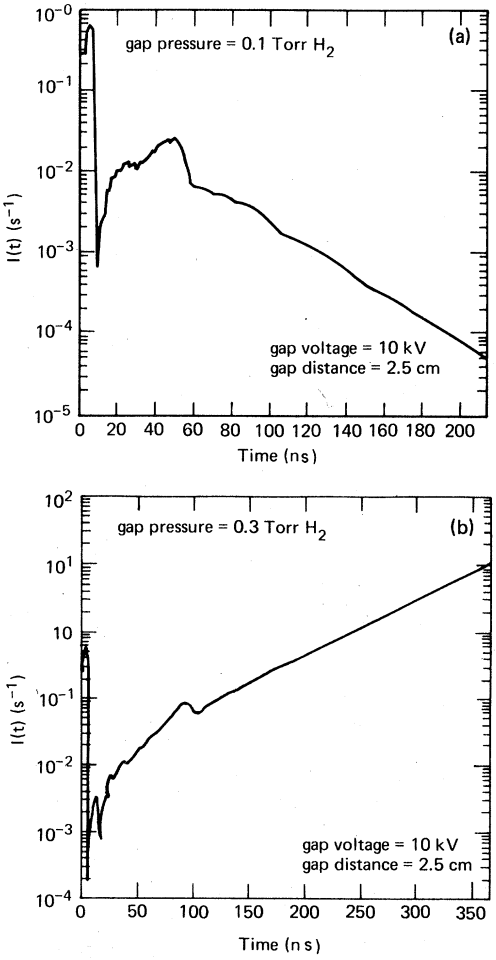

FIG. 5. (a) Rate of electron emission at cathode versus time (decay at 10 kV and 0.1 Torr). (b) Rate of electron emission at cathode versus time (growth at 10 kV and 0.3 Torr).

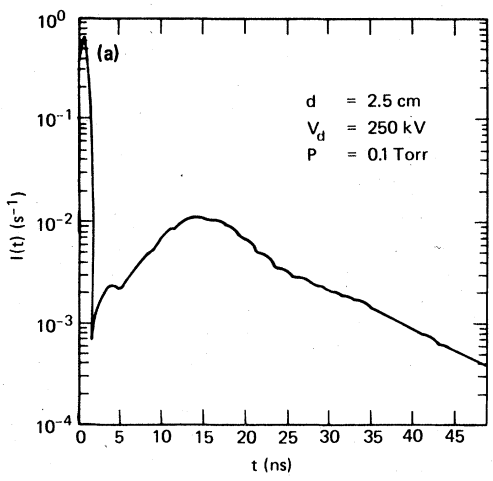

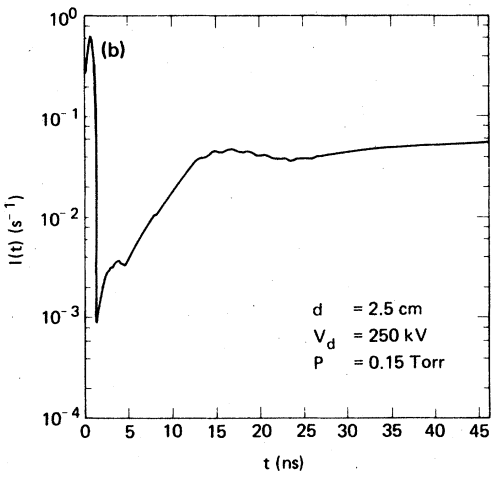

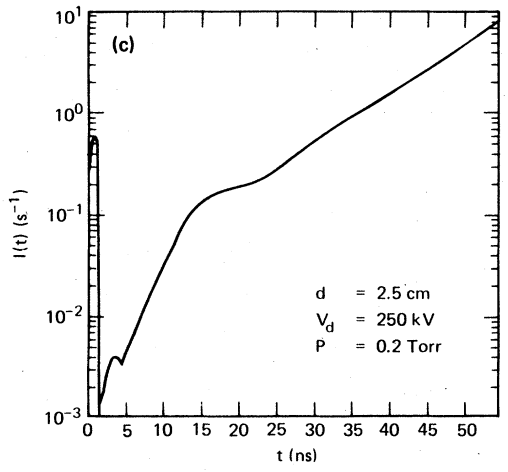

FIG. 6. (a) Rate of electron emission at cathode versus time (at 250 kV and 0.1 Torr). (b) Rate of electron emission at cathode versus time (at 250 kV and 0.15 Torr). (c) Rate of electron emission at cathode versus time (at 250 kV and 0.2 Torr).

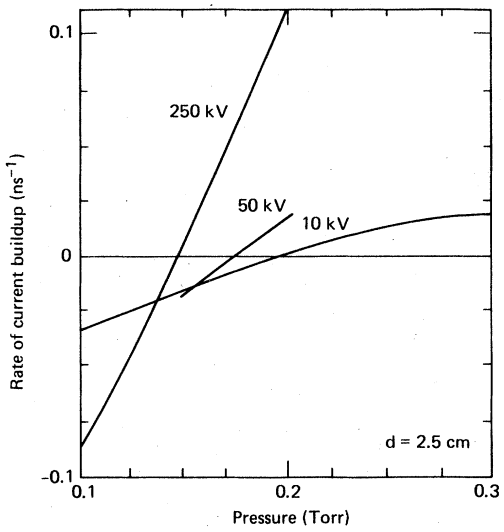

FIG. 7. Rate of current buildup versus gas pressure for three gap voltages.

approximation.

In Fig. 4, we show the rate of electron emission from the cathode as a function of time. The initial peak in $I(t)$ is due to the externally supplied trigger (which is a Gaussian with a width of 6 ns). After the initial trigger has been turned off, $I(t)$ goes through a short phase of somewhat unsystematic variations as R_i and R_0 make rapid adjustments in response to the initial trigger. However, beyond this phase, $I(t)$ smooths out into a simple exponential in time as R_i and R_0 settle into some relatively constant shapes. For this particular run (at $P = 0.2$ Torr), $I(t)$ is nearly constant asymptotically. The asymptotic behavior of $I(t)$ changes to simple exponential decay at 0.1 Torr [Fig. 5(a)] and a simple exponential growth at 0.3 Torr [Fig. 5(b)]. Similar plots of $I(t)$ at a higher gap voltage of $V_d = 250$ kV, with the same gap distance of 2.5 cm, are shown in Figs. 6(a) through 6(c). Again, we see that the asymptotic behavior of $I(t)$ changes from a simple decay to a near constant to an exponential growth as the pressure changes from 0.1 Torr to 0.15 Torr to 0.2 Torr, respectively. These plots permit us to derive a precise value for the growth rate $\nu(p)$, where $I(t) \sim \exp(\nu t)$ as $t \to \infty$. Self-breakdown is predicted to take place if ν is positive.

Results from several runs at three different gap voltages are summarized on plots of the growth rate ν as a function of pressure in Fig. 7. All runs were made at a gap distance of 2.5 cm. The points at which the curves cross the $\nu = 0$ axis give the critical pressure for self-breakdown. Overall, the magnitude of the growth rates is larger at higher gap voltages. This is not sur-

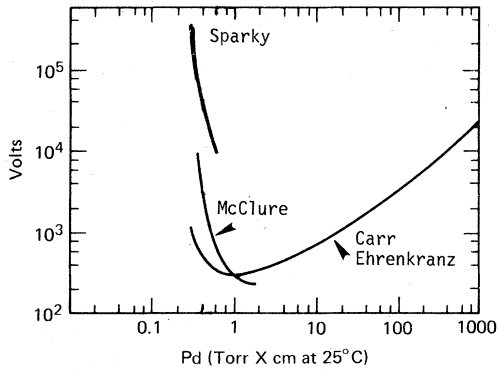

FIG. 8. Hydrogen breakdown voltage versus Pd including: SPARKY model predictions, measurements by McClure (Ref. 12) and measurements by Carr and Ehrenkranz (Ref. 13).

prising since at the higher voltages the ions and neutrals move much faster.

The critical pressures ($\nu = 0$) at various gap potentials are plotted on a Paschen curve in Fig. 8. For comparison, we have plotted on the same figure previous measurements at both the high- and the low-pressure end. While there are no known measurements to date at the high-gap voltages for which our calculations were performed, we do see a consistent trend between our predictions and previous data. One notes that in going from 10 kV to 250 kV, the change in the predicted critical Pd is not large.

Implicit in the concept of the Paschen curve is the assumption that the critical pressure is inversely proportional to the gap distance. This simple scaling is not obvious from our theory. In fact, several terms in Eqs. (C1) to (C3) break Pd scaling explicitly. Results at two different gap distances of $d = 2.5$ cm and $d = 1$ cm are shown in Fig. 9. At both gap voltages, the curves at the two gap distances are seen to cross at around $\nu = 0$. This is an explicit verification of Pd scaling. It is interesting to note, however, that the growth

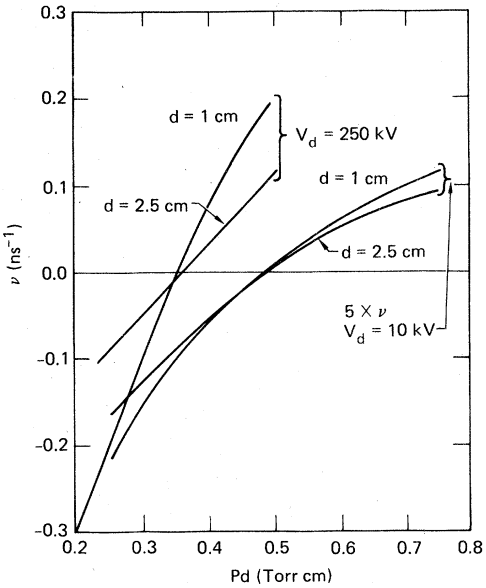

FIG. 9. Buildup rate vs Pd at two gap distances and two gap potentials.

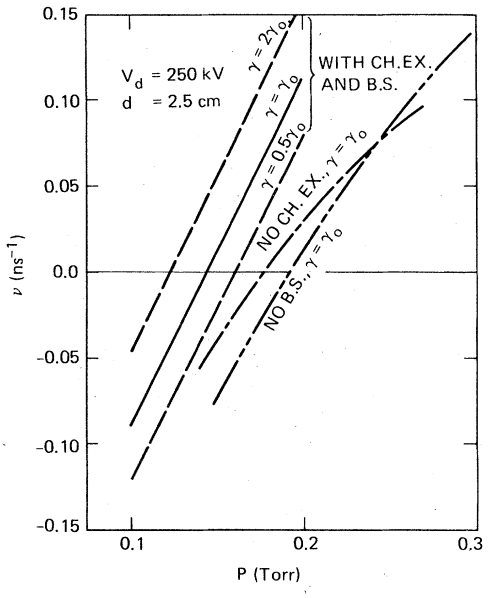

FIG. 10. Buildup rate vs Pd at 250 kV, effect of varying γ, turning off charge exchange and turning off backscatter.

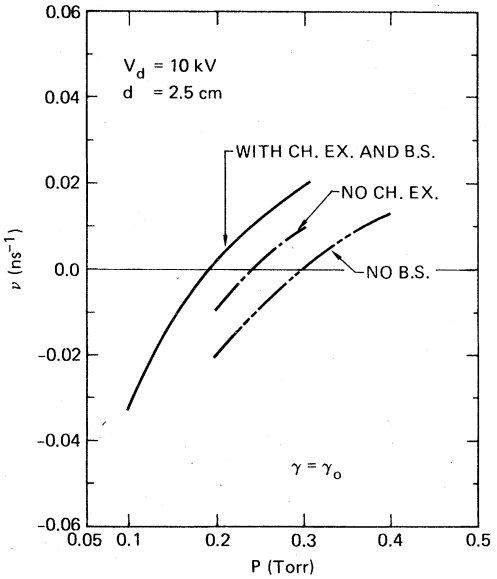

FIG. 11. Buildup rate vs Pd at 10 kV, effect of turning off charge exchange and of turning off backscatter.

rates away from the critical point do not scale with Pd.

To ascertain the sensitivity of the final results to various physical processes, we have performed a series of runs with backscatter or neutral effects turned off. The resulting growth rates are shown in Figs. 10 and 11. It is not surprising that by turning off these effects, the growth rate $\nu(P)$ is decreased consistently.

Since the secondary-electron emission coefficient γ is known to be sensitive to the smoothness of the electrode surface, we have also done some tests by varying γ. It is seen from Fig. 10 that decreasing or increasing γ by a factor of 2 produces a relatively minor effect on the growth rates.

ACKNOWLEDGMENTS

Lawrence Livermore National Laboratory is operated by the University of California for the Department of Energy under Contract W-7405-ENG-48. This work is performed by Lawrence Livermore National Laboratory for the Department of Defense under DARPA (DOD) ARPA Order 3178, Amendment No. 12, monitored by NSWC under Contract No. N60921-80-PO-WO188.

APPENDIX A: MODIFIED-MEAN-FREE-PATH MODEL FOR CHARGE EXCHANGE OF ENERGETIC IONS

The charge-exchange cross section for H_2^+ is a slowly varying function of ion energy for $T_i \lesssim 10$ keV. However, at higher energies, the cross section is substantially reduced. If the potential across the gap is low (e.g., $V_d = 10$ kV), the constant-mean-free-path assumption is valid. But at higher potentials (e.g., $V_d = 250$ kV), ions can be accelerated to much higher energies. The energetic ions have a reduced probability for charge transfer, and may be considered as approaching free-fall conditions.

To treat the effect of energetic escaping ions, a modification of the mean-free-path approximation is introduced. Over a characteristic length λ_c for charge exchange, the ion is viewed as having a finite probability G of charge exchange, and the probability $(1-G)$ of escape. To calculate λ_c and G, we note that ion loss due to charge exchange is given by

$$dN = -N(x) n_g \sigma_c \left(\frac{eV_d x}{d}\right) dx \,. \tag{A1}$$

The probability G is then

$$G = \frac{N(0) - N(\infty)}{N(0)} = 1 - \exp\left(-n_g \int_0^\infty \sigma_c dx\right), \tag{A2}$$

while the characteristic length is

$$\lambda_c = \frac{\int dx\, dN}{\int dN} \,. \tag{A3}$$

Since only a fraction of the total ions will charge exchange, the neutral production rate is reduced, and Eq. (8) is modified to give

$$R_0(t,x) = \sum_{m=1}^{M} G^m R_i(t - mt_0, x + m\lambda_c) \,. \tag{A4}$$

The energetic ions as well as the slow ions will impinge upon the cathode to release secondary electrons. The contributions from both types of ions must be included in Eq. (4). The contribution from the slow ions is given by

$$\int_0^d dx' G^m R_i(t - t_i, x') \gamma(T_i) \,, \tag{A5}$$

where $m\lambda_c \leq x' < (m+1)\lambda_c$.

The weighting factor of G^m accounts for the reduction of impinging slow ions due to escape. There is a similar contribution from the fast ions. The fraction of ions which escape after n charge exchanges ($n < m$) is weighted by the factor $(1-G)\,G^n$. The time delay and the ion energy at the cathode of the escaping ions can be calculated as before. Finally, one must perform the sum over n. Modification of the electron-ion-pair production rate equation proceeds analogously, with contributions from both the fast and the slow ions.

APPENDIX B: IONIZATION BY BACKSCATTERED ELECTRONS

In this appendix, the production rate of electrons is calculated at a point x in the gap due to backscattered electrons. Electrons originally produced at point x' (see Fig. 1) impinge upon the anode with kinetic energy $T' = eV_d(d - x')/d$. The electrons are reflected with a distribution in angle as well as in energy $T'' \leq T'$. We assume the distribution in solid angle to be simply proportional to $\cos\theta$, and that the reflected distribution is a function of the ratio T''/T', but otherwise independent of the incident energy T'. The reflection coefficient $\eta(T''/T')$ is a measured quantity and is defined such that the total fraction of reflected electrons is given by

$$\frac{N_{\text{reflected}}}{N_{\text{incident}}} = \int_0^{\pi/2} 2\pi \sin\theta\, d\theta \times \int_0^1 d\left(\frac{T''}{T'}\right)\left[\cos\theta\,\eta\left(\frac{T''}{T'}\right)\right]. \tag{B1}$$

A reflected electron with energy T'' at an angle θ will traverse a parabolic trajectory, again assuming frictionless motion in a constant force field. If the trajectory crosses the point x, it will

have a finite probability of ionization in a slab of length dx which is given by

$$2n_g\sigma_e(T''-T)ds = 2n_g\sigma_e(T''-T)\frac{ds}{dx}\,dx\,. \qquad \text{(B2)}$$

The factor 2 enters because the parabolic trajectory will intersect the slab at x twice, once while it is moving away from the anode, and once while it is falling back towards the anode. The energy of the electron at the point x is given by

$$T''-T = T''-\frac{eV_d}{d}(d-x)\,. \qquad \text{(B3)}$$

Simple consideration of the kinematics gives

$$\frac{ds}{dx}=\frac{ds/dt}{dx/dt}=\frac{v}{v_x}$$

$$=\left(\frac{T''-T}{T''\cos^2\theta-T}\right)^{1/2}H(T''\cos^2\theta-T)\,, \qquad \text{(B4)}$$

where H is the step function.

We are now ready to calculate the contribution to R_i from the backscattered electrons. Consider first the contribution from electrons which originate from the cathode ($x'=0$). In this case, electrons impinge upon the anode with energy $T'=eV_d$. The contribution to the electron production rate at x is then given by

$$R_i(t,x)=I(t)n_gF(eV_d,T)\,, \qquad \text{(B5)}$$

where

$$F(T',T)=\int_0^{\theta_{\max}}2\sin\theta\,d\theta \times\int_{(T''/T')_{\min}}^{1}d\left(\frac{T''}{T'}\right)\eta\left(\frac{T''}{T'}\right)\cos\theta\,2\sigma_e(T''-T')\frac{ds}{dx}\,. \qquad \text{(B6)}$$

In addition, there is an analogous contribution from electrons which originate in the gap

$$R_i(t,x)=\int_0^x dx'R_i(t,x')n_gF(T',T)\,. \qquad \text{(B7)}$$

We note in Eq. (B7) that only electrons originally produced at $x'\leq x$ can contribute at x via backscattering.

$F(T',T)$ has the dimension of cm^2, and can be viewed in some sense as an effective ionization cross section by backscattered electrons. We can reduce Eq. (B6) further by explicitly performing the angular integration. This yields

$$F(T',T)=\frac{4\pi}{T'}\int_T^{T'}dT''\sigma_e(T''-T)\eta\left(\frac{T''}{T'}\right)\left(\frac{T''-T}{T''}\right). \qquad \text{(B8)}$$

This expression is an integral over two measured quantities, the cross section for ionization and the reflection coefficient η. $F(T',T)$ is evaluated numerically in SPARKY.

APPENDIX C: SUMMARY OF EQUATIONS SOLVED BY SPARKY

We summarize here the entire set of equations solved by the numerical code SPARKY. Some notations have been changed from the text for convenience, but are internally consistent within this appendix.

Independent Variables.

t = time,
x = distance from the cathode.

Externally Specified Parameters.

V_d = gap voltage,
d = gap distance,
n_g = density of gas,
$S(t)$ = source function (triggered electron emission).

Calculated Quantities.

$I(t)$ = rate of secondary electron emission,
$R_0(t,x)$ = rate of neutral production in the gap,
$R_i(t,x)$ = rate of electron-ion pair production in the gap.

Atomic Data.

γ = coefficient for secondary electron emission,
σ_e = ionization cross section by electron impact,
σ_i = ionization cross section by ion impact,
σ_0 = ionization cross section by neutral impact,
σ_c = charge-exchange cross section,
η = reflection coefficient.

Constants.

M = molecular mass,
e = electronic charge.

Rate of Cathode Electron Emission.

$$I(t)=S(t)+\gamma(T_c)\int_0^d dx'R_0\left(t-\frac{x'}{v_c},x'\right) + \int_0^d dx'\left((1-G)\sum_{n=0}^{m-1}R_i(t-t_n^0,x')\gamma(T_n^0)G^n+R_i(t-t_m^0,x')\gamma(T_m^0)G^m\right), \qquad \text{(C1)}$$

where

$$m\lambda_c \leq x' < (m+1)\lambda_c ,$$

$$t_n^0 = nt_c + \left(\frac{2M}{eE}(x' - n_c)\right)^{1/2} ,$$

$$T_n^0 = eE(x' - n\lambda_c) ,$$

$$T_c = eE\lambda_c ,$$

$$v_c = (2T_c/M)^{1/2} ,$$

$$t_c = (2M\lambda_c/eE)^{1/2} ,$$

$$\lambda_c = \frac{1}{G}\int_0^\infty dx\, x n_g \sigma_c(eEx) \exp\left(-n_g \int_0^x dx' \sigma_c(eEx')\right) ,$$

$$G = 1 - \exp\left(-n_g \int_0^\infty dx\, \sigma_c(eEx)\right) ,$$

and

$$E = V_d/d .$$

Rate of Neutral Production in the Gap.

$$R_0(t,x) = \sum_{n=1}^{\bar{m}} G^n R_i(t - nt_c, x + n\lambda_c) ,$$

where

$$\bar{m}\lambda_c \leq d - x < (\bar{m}+1)\lambda_c .$$

Rate of Electron-Ion-Pair Production in the Gap.

$$\begin{aligned} R_i(t,x) = {} & I(t) n_g \sigma_e(eEx) + \int_0^x dx' R_i(t,x') n_g \sigma_e[eE(x - x')] + I(t) n_g F[eEd, eE(d - x)] \\ & + \int_0^x dx' R_i(t,x') n_g F[eE(d - x'), eE(d - x)] + \int_x^d dx' R_0\left(t - \frac{x' - x}{v_c}, x'\right) n_g \sigma_0(T_c) \\ & + \int_x^d dx' \left((1 - G)\sum_{n=0}^{\tilde{m}-1} R_i(t - t_n, x' - x) n_g \sigma_i(T_n) G^n + R_i(t - t_{\tilde{m}}, x' - x) n_g \sigma_i(T_{\tilde{m}}) G^{\tilde{m}}\right) , \end{aligned} \tag{C3}$$

where

$$F(T', T) = \frac{4\pi}{T'}\int_T^{T'} du \left(\frac{u - T}{u}\right) \sigma_e(u - T)\eta\left(\frac{u}{T'}\right) ,$$

$$\tilde{m}\lambda_c \leq x' - x < (\tilde{m}+1)\lambda_c ,$$

$$t_n = nt_c + \left(\frac{2M}{eE}(x' - x - n\lambda_c)\right)^{1/2} ,$$

and

$$T_n = eE(x' - x - n\lambda_c) .$$

[1] S. S. Yu, E. J. Lauer, and D. M. Cox, 32nd Annual Gaseous Electronics Conference, Pittsburgh, Pennsylvania (1979), Abstract DB-5 (unpublished).

[2] A. J. Dempster, Phys. Rev. 46, 728 (1934).

[3] K. D. Grarzow and G. W. McClure, Phys. Rev. 125, 1792 (1962).

[4] D. Bhasavanich and A. B. Parker, Proc. R. Soc. London Ser. A 358, 385 (1977).

[5] C. F. Barnett, J. A. Ray, E. Ricci, M. I. Wilker, E. W. McDaniel, E. W. Thomas, and H. B. Gilbody, Oak Ridge National Laboratory Report ORNL 5207 (1977), Vol. II, D3.10.

[6] L. N. Large and W. S. Whitlock, Proc. Phys. Soc. London 79, 148 (1962).

[7] C. F. Barnett, J. A. Ray, E. Ricci, M. I. Wilker, E. W. McDaniel, E. W. Thomas, and H. B. Gilbody, Oak Ridge National Laboratory Report ORNL 5207 (1977), Vol. II, C4.8.

[8] C. F. Barnett, J. A. Ray, E. Ricci, M. I. Wilker, E. W. McDaniel, E. W. Thomas, and H. B. Gilbody, Oak Ridge National Laboratory Report ORNL 5206 (1977), Vol. I, A5.26.

[9] C. F. Barnett, J. A. Ray, E. Ricci, M. I. Wilker, E. W. McDaniel, E. W. Thomas, and H. B. Gilbody, Oak Ridge National Laboratory Report ORNL 5206 (1977), Vol. I, A4.30.

[10] H. Kulenkampff and W. Spyra, Z. Phys. 137, 416 (1954).

[11] W. C. Walker, O. P. Rustgi, and G. L. Weissler, J. Opt. Soc. Am. 49, 471 (1959).

[12] G. W. McClure, J. Electron. Control 7, 439 (1959).

[13] J. M. Meek and J. D. Craggs, *Electrical Breakdown in Gases* (Clarendon, Oxford, 1953), Fig. 2.2.